Research in Pharmaceutical Sciences, December 2015; 10(6): 504-513
Received: Jan 2015
Accepted: Mar 2015

School of Pharmacy & Pharmaceutical Sciences
Isfahan University of Medical Sciences

***Original Article***

# Synthesis of some new porphyrins and their metalloderivatives as potential sensitizers in photo-dynamic therapy

**Mahboubeh Rostami[1], Leila Rafiee[2], Farshid Hassanzadeh[1,*], Ali Reza Dadrass[2], and Ghadam Ali Khodarahmi[1]**

*[1]Department of Medicinal Chemistry, School of Pharmacy and Pharmaceutical Sciences and Isfahan Pharmaceutical Sciences Research Center, Isfahan University of Medical Sciences, Isfahan, I.R. Iran.*
*[2]Department of Chemistry, Faculty of Science, Urmia University, Urmia 57153, I.R. Iran.*

## *Abstract*

Porphyrins are a ubiquitous large class of naturally occurring macrocyclic compounds with many significant biological representatives comprising heme and chlorophyll. Some novel adaptable methods for the synthesis of free-based porphyrins as promising sensitizers for the use in photo-dynamic therapy by the virtue of their known tumor affinity, low dark cytotoxicity, and easy synthesis in good to high yields have already been discussed. In the present study, two new porphyrins including TAPFA, as a novel folic acid targeted porphyrin sensitizer, and TAP-Schiff base, as a novel sensitizer with better light absorption, were prepared for the first time and their structures were confirmed by $^{1}$H NMR, $^{13}$C NMR, FT-IR and UV-Vis spectroscopy as well as CHNS analysis . The compounds were metalized with Zn(II) and Fe(II) metal ions to study how the metal ions can improve the light absorption wavelength and their water solubility. The structures of metalized compounds were also confirmed by FT-IR and UV-Vis spectroscopy.

***Keywords:*** Porphyrins; Metalloporphyrins; Photo-dynamic therapy (PDT); Two-photon absorption (TPA)

## INTRODUCTION

In recent years, synthesis and study of porphyrin systems has gained special attention due to their unique physical, chemical, and spectroscopic properties making them very interesting materials for application in molecular electronic devices (1) and catalysis (2,3). In addition, porphyrin compounds can be effective as sensitizing agent for diagnosis and photodynamic therapy (PDT) of cancers (4) that has achieved great deal of interest as an effective alternate for chemotherapy owing to their non-invasive nature (5,6). PDT is predicated on the activation of a tumor-localized sensitizer with light of definite wavelength, and production of lethal toxic agents such as the reactive oxygen species (ROS) to kill the cancer cells (Fig. 1) (7,8). In this regard, an ideal photosensitizer agent should have some special properties like water-solubility, light absorption efficacy (photo reactive), and light absorption peak around visible to near-infrared region of electromagnetic spectrum. In recent years two water insoluble porphyrin derivatives VerTAPrphyrin and Hematoporphyrin derivatives have b approval by the FDA for clinical PDT (9).

PDT employs the special ability of porphyrin photosensitizers to accumulate in pathologic cells and to produce extremely active and lethal singlet oxygen molecules due to the absorption of photon energy, which then spread out the surrounding tumor. Unfortunately, the limited diffusion depth of visible light into the biological tissues allows only few types of accessible cancers (like skin and breast) to be treated in this way. To make PDT more generally applicable, it is essential to deliver light deeper into the tissue. This might be achieved by employing the nonlinear-optical impact of two-photon absorption (TPA) in which case the illumination is carried out at near-infrared (IR) sub spectrum wavelengths, whenever the tissue is considerably more permeable to the visible region wavelengths. However, to this point, TPA of tumor-specific porphyrin sensitizers has been really ineffective.

*Corresponding author: F. Hassanzadeh
Tel: 0098 31 37927096, Fax: 0098 31 36680011
Email: hassanzadeh@pharm.mui.ac.ir

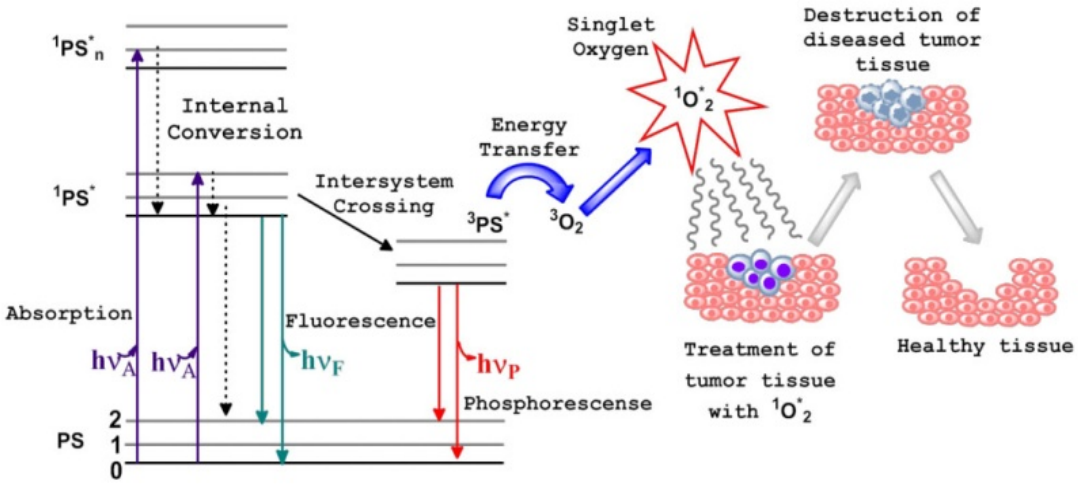


**Fig. 1.** Mechanism of photodynamic therapy.

This would result in the impractical treatment of deeper tumors (10) and along with this ideal purpose, here; we introduce a new porphyrin photosensitizer [tetra-amino porphyrin (TAP)-Schiff base] with an increased TPA cross-section due to its more delocalized structure beside its two metal complexes (zinc tetra-amino porphyrin (ZnTAP)-Schiff base and ferrous tetrakis-amino porphyrin (FeTAP)-Schiff base).

On the other hand, the main drawback of most applicable photosensitizers in PDT is the lack of their selectivity towards cancerous cells which leads to the destruction of healthy cells during the treatment. Practically, some modifications such as the attachment of a targeting group as cancer tracer molecule on the drug structure could result in the specific therapy of the tumor tissues. Therefore, various targeting agents including peptides, hormones, vitamins, folic acid (FA), and monoclonal antibodies have been utilized for drug targeting (11).

The over expression of folate receptors in a number of carcinomas including ovary, brain, kidney, breast, colon and lung (12–14) has been confirmed and owing to this high expression, the foremost difficult cancer cells to treat in classical methods can be effectively targeted with FA conjugated therapeutics (15,16).

Except the two porphyrin-FA conjugates reported by Li and coworkers (17) and Scheider and colleagues (18), there are not many reports on the synthesis of photosensitizers conjugated with folic acid. On the other words, no reports on the direct covalent linkage between aminoporphyl compounds with FA are available in the literatures. This work reports on an amide chemical bonding between TAP, ZnTAP, FeTAP, and FA to form TAPFA, ZnTAPFA, and FeTAPFA conjugates (Fig. 2). In all cases, water solubility of the compound which is a vital parameter for their biological activity was improved by metallation.

Nowadays, investigation of biomimetic reactions is very interesting to the point that a variety of synthetic metalloporphyrin derivatives have been demonstrated to be efficient as model systems for many life processes and enzyme actions (19–25). One of the most important studies of the metalloporphyrins is their utilization as a model for some natural enzymes such as peroxidase enzyme in which the activation of dioxygen is obtained by metalloporphyrin catalysts under mild conditions (26). In this regard, the iron porphyrin complexes are widely used as model compound to simulate the catalytic mechanism of cytochrome P450 enzymes in biological processes (27).

In the current study, for the first time, we report on the effective synthesis of some novel porphyrins and their metalized derivatives that, due to their specific targeting to cancerous cells and resonance expanding moiety as a Schiff base structure, can be effectively used in PDT. These novel structures are the basis of some other ongoing researches in this laboratory.

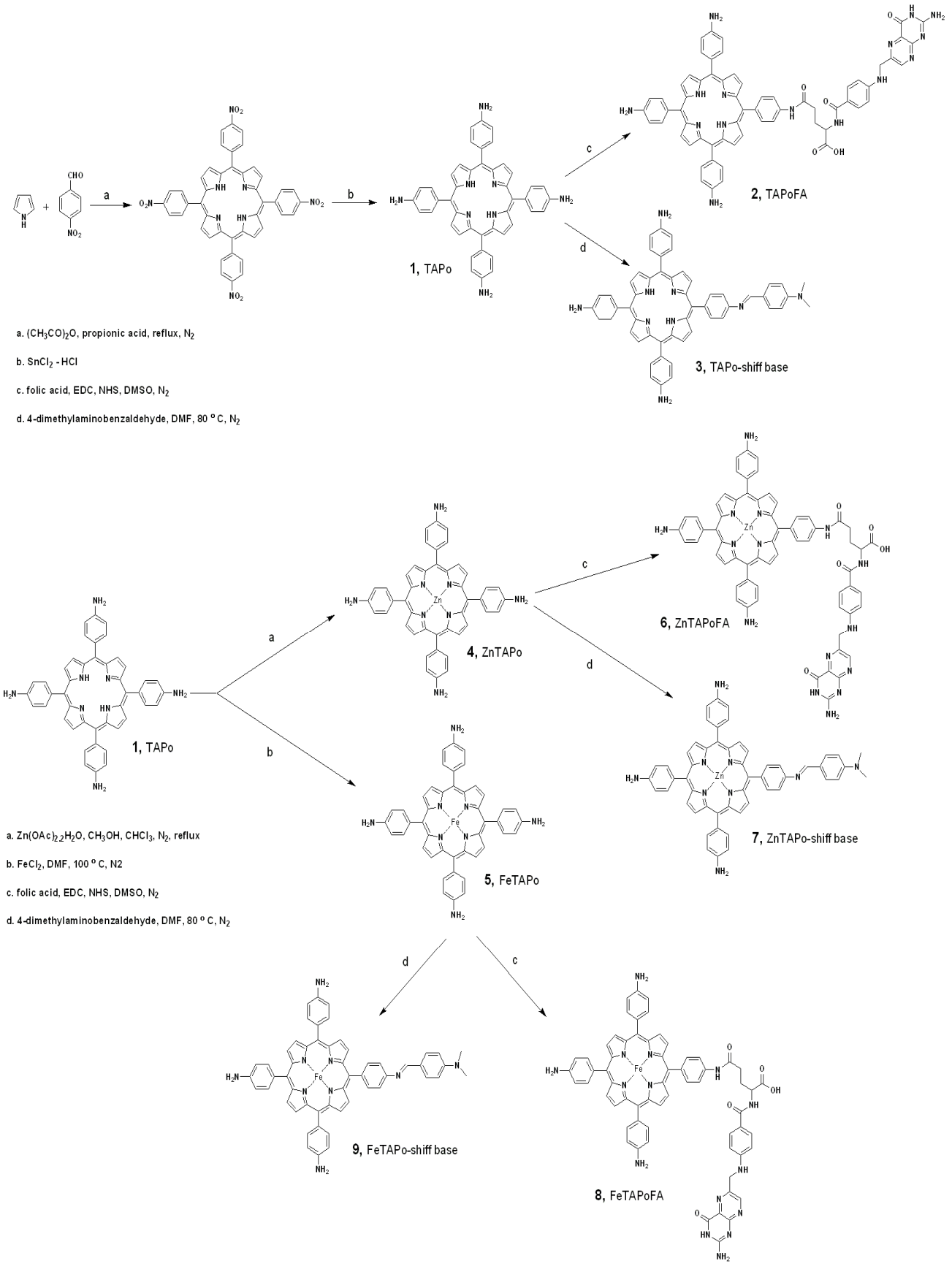


**Fig. 2.** Synthesis of porphyrin compounds.

## MATERIALS AND METHODS

### *Chemistry*

All chemicals used for the synthesis of the compounds were purchased from Merck or Sigma. 3-(ethyliminomethyleneamino)-N,N-dimethylpropan-1-amine (EDC) and 1-Hydroxy-2,5-pyrrolidinedione (NHS) were supplied by Sigma Co. and used without further purification. Pyrrole was redistilled before the use. The purity of the compounds was investigated by thin layer chromatography (TLC) on silica gel plate using appropriate solvents. The progress of all chemical reactions was controlled by TLC as described. Ultraviolet-visible (UV-Vis) spectra were obtained on Perkin Elmer EZ201- (USA). The IR spectra were recorded with a WQF-510 ratio recording fourier transform infrared (FTIR) spectrometer (China) using a KBr disc ($\gamma$, $cm^{-1}$). The NMR spectra were recorded using a Brucker 400 MHz spectrometer (Germany) and dimethyl sulfoxide (DMSO)-d6 was used as solvent. Chemical shifts ($\delta$) are revealed in ppm downfield from the internal standard tetramethylsilane. All porphyrin derivatives were synthesized according to the procedure shown in Fig. 2.

### *Synthesis of 5,10,15,20-meso-tetrakis(p-aminophenyl) porphyrin, TAP,* **1**

A mixture of p-nitrobenzaldehyde (34 mmol, 5.27 g) and acetic anhydride (64 mmol, 6 ml) was added to 150 ml of propionic acid while stirring under nitrogen atmosphere and the resulting solution was heated to reflux. To this, a freshly distilled pyrrole (34 mmol, 2.34 g) in 5 ml of propionic acid was added and the mixture was refluxed for further 30 min while stirring. The tarry solution was allowed to cool and kept for further 24 h. The dark solid was collected by filtration, washed with six 50 ml portions of $H_2O$, and dried under vacuum. The powdery solid was mixed with 40 ml of pyridine, refluxed under stirring for 1 h, cooled to room temperature, and then stored at –4 °C overnight. The tarry mixture was filtered and the solid product washed repeatedly with acetone until the rinsing was no longer dark yielding 1.95 g (24%) of 5,10,15,20-meso-tetrakis(p-nitrophenyl)porphyrin. A solution of 5, 10, 15, 20 - meso - tetrakis(p-nitrophenyl) porphyrin (2.5 mmol, 2 g) in 100 ml of concentrated HC1 was bubbled with Ar for 1 h. A solution of $SnC1_2.2H_2O$ (40 mmol, 9 g) in 10 ml of concentrated HC1 also bubbled with $N_2$, was added to the porphyrin solution. The resulting mixture was stirred and heated in a water bath (75-80 °C) for 30 min. The hot-water bath was carefully replaced with a cold-water bath and then an ice-bath (-5 °C). The reaction mixture was then neutralized under Ar by slow addition of 110 ml of concentrated $NH_40H$, taking care to maintain a low temperature throughout the very exothermic reaction. The resultant basic solution was exposed to air and filtered and the greenish solid stirred vigorously with 200 ml of 5% NaOH. The obtained solid was again filtered, washed with water, dried, and then Soxhlet extracted with 250 ml of $CHC1_3$. The volume of the purple solution was reduced to 150 ml by rotary evaporation. Addition of 100 ml of 95% EtOH and slow rotary evaporation gave crystalline tetra aminophenyl porphyrin, TAP, yield about 1.0 g (50%). The structure of pure final product was confirmed by hydrogen-1 nuclear magnetic resonance ($^1$H NMR), 13C nuclear magnetic resonance ($^{13}$C NMR), FTIR spectroscopy, CHNS analysis. Electron transfer pattern was evaluated by UV-Vis spectroscopy.

### *Synthesis of TAPFA, 2*

To a stirring solution of FA (0.167 mmol, 74 mg) in 2 ml of anhydrous DMSO under $N_2$ atmosphere was added EDC (0.25 mmol, 48 mg), NHS (0.25 mmol, 29 mg) and the mixture was stirred for further 4 h at room temperature. This solution was added drop wise to a solution of TAP (0.167 mmol, 0.113g) in 5 ml of anhydrous DMSO, and stirred for 48 h at room temperature under nitrogen atmosphere. The progress of the reaction was monitored by TLC, till no porphyrin detected. The reaction was stopped by the addition of 10 ml ethyl acetate. The resulting precipitate were filtrated and dried under vacuum, yield 0.178 g (63.5%) of desired product. The structure of pure final product was confirmed by $^1$H NMR, $^{13}$C NMR, FTIR spectroscopy, and CHNS analysis and changes in the behavior of electron transfers were studied by UV-Vis spectroscopy.

***Synthesis of TAP-Schiff base, 3***

TAP 1 (0.2 mmol, 135 mg) and 4-dimethylaminobenzldehyde (0.2 mmol, 30 mg) were dissolved in 10 ml of dry toluene containing 4 Å molecular sieves. The resulting solution was refluxed until the disappearance of the TAP 1 and monitored by TLC (24 h). The solvent was removed under reduced pressure and the crude product was dissolved in $CH_2Cl_2$ and filtered. Evaporation of the solvent gave purple solids. The product was recrystallized from $CH_2Cl_2$ and light petroleum (yield, 75%). The structure of pure final product was confirmed by $^1H$ NMR, FTIR spectroscopy, and CHNS analysis and also in this case, the effects of more electron delocalization compared to the initial TAP were estimated by UV-Vis spectroscopy.

***Synthesis of ZnTAP, 4***

TAP 1 (0.14 mmol, 95 mg) and Zn $(CH_3COO)_2$ (1.08 mmol, 0.198 g) were dissolved in a mixture of methanol and chloroform under $N_2$ atmosphere. The mixture was refluxed for 4 h at 65 °C. After completion of the reaction, the solvent was removed and the crude product was purified by recrystallization in ethanol to give 4 Yield, 90 %. The structure of this complex and changes in the electron transfer pattern were characterized by FTIR and UV-Vis spectroscopy respectively.

***Synthesis of FeTAP, 5***

To the solution of 0.2 mmol of TAP in 30 ml dimethylformamide, 2 mmol of $FeCl_2.4H_2O$ in three portions was added over 30 min. The mixture was heated and the reaction process was monitored by TLC whenever possible. When TLC indicated the disappearance of free base porphyrin, the reaction was stopped. The resulting mixture was cooled to 50 °C–60 °C and 40 ml HCl (6 M) was added to the solution to give a precipitate. The solution was filtered and washed with 1 M of HCl until the filtrate no longer appeared green. The resulting solid was vacuum-dried and afforded above 90% yield of FeTAP. The structure of this porphyrin complex was characterized by FIR and the electron transfer pattern and its changes relative to the corresponding porphyrin were studied by UV-Vis spectroscopy.

***Synthesis of ZnTAPFA, 6***

EDC (0.3 mmol, 58 mg) and NHS (0.3 mmol, 35 mg) were added to a stirring solution of FA (0.2 mmol, 88 mg) in 5 ml of anhydrous DMSO under $N_2$ atmosphere and the mixture was stirred for further 4 h at room temperature. The resulting solution was added drop wise to a solution of ZnTAP 4 (0.2 mmol, 0.148 g) in 5 ml anhydrous DMSO and stirring was continued for 48 h at room temperature under nitrogen atmosphere. The progress of the reaction was monitored by TLC, till no porphyrin detected and the reaction was stopped by the addition of 10 ml of ethyl acetate. The resulting precipitates were filtrated and dried under vacuum to obtain desired product (yield, 73%). The structure of pure final product and acceptable changes in the light absorption pattern were confirmed by FTIR and UV-Vis Spectroscopy respectively.

***Synthesis of ZnTAP-Schiff base, 7***

ZnTAP 4 (0.2 mmol, 0.148 g) and the 4-dimethylaminobenzldehyde (0.2 mmol, 30 mg) were dissolved in 10 ml of dry toluene containing 4 Å molecular sieves. The resulting solution was refluxed until the disappearance of the ZnTAP 4 and monitored by TLC (48 h). The solvent was removed under reduced pressure and the crude product was dissolved in $CH_2Cl_2$ and filtered. Evaporation of the solvent gave purple solids that were further purified by recrystallization from $CH_2Cl_2$ and light petroleum. Also, the structure of pure final product and acceptable changes in the light absorption pattern were confirmed by FTIR and UV-Vis spectroscopy respectively.

***Synthesis of FeTAPFA, 8***

The activated FA was added to the solution of FeTAP in DMSO and the workup condition was the same as described for the synthesis of ZnTAPFA, **6**. As described for other derivatives, the characterization of pure metalloporphyrin and its electron transfer behavior were studied by FTIR and UV-Vis spectroscopy.

***Synthesis of FeTAP-Schiff base, 9***

As described for the synthesis of ZnTAP-Schiff base,**7**, 4-dimethylaminobenzldehyde was added to the solution of FeTAP in DMSO and the workup condition was set as reported for **7**.

**Table 1.** UV-Vis data of base porphyrins and metalated porphyrins.

| Entry | Compound | λ (max) | |
|---|---|---|---|
| | | Soret band | Q band |
| 1 | TAP | 427 | 521, 565, 592, 660 |
| 2 | TAPFA | 429 | 522, 565, 593, 660 |
| 3 | TAP-Schiff base | 466 | 525, 566, 602, 661 |
| 4 | ZnTAP | 430 | 560, 604 |
| 5 | FeTAP | 429 | 543, 585 |
| 6 | ZnTAPFA | 432 | 550, 590 |
| 7 | ZnTAP-Schiff base | 475 | 530, 580 |
| 8 | FeTAPFA | 431 | 530, 580 |
| 9 | FeTAP-Schiff base | 468 | 528, 570 |

## RESULTS

### *Chemistry*

The TAP was prepared in a relatively high yield with the primary condensation of 4-nitrobenzaldehyde and pyrrole in refluxing propionic acid and in continue, reducing the nitro group to amino moiety with $SnCl_2$-HCl as catalyst. TAPFA and TAP-Schiff base were prepared by the reaction of the appropriate quantities of activated FA and 4-dimethylaminobenzaldehyde in good yields. Matalloporphyrins (ZnTAP, FeTAP) and their corresponding folate targeted and Schiff bases (ZnTAPFA, FeTAPFA, ZnTAP-Schiff base and FeTAP-Schiff base) were prepared from the reaction of metalloporphyrin produced primarily with the reaction of porphyrin with desired metal salt in a simple and effective procedure and consequently with FA or 4-dimethylaminobenzaldehyde (Fig. 2).

The structures of all compounds were investigated and confirmed by FTIR and NMR spectroscopy. To study how the metallation or substitution on porphyrin structure can affect its photophysical properties, in all cases, the UV–Vis spectra were obtained and compared. For further and more precise characterization, we analyzed the C, H and N content of three porphyrins base with CHNS analysis method. The details of the spectral data for the prepared compounds are provided as below:

**TAP, 1:** FTIR: (KBr) $\gamma cm^{-1}$: 3424 (NH str.), 3364 (NH str.), 1600 (N-H deformation), 1469 (C=C aromatic); $^1$H NMR (DMSO-D6); δ ppm: 8.81 (s, 8H, β pyrrole) ,7.85 (d, 8.40 Hz, 8H, protons meta to the $NH_2$), 7.00 (d, 8.40 Hz, 8H, ortho protons to the $NH_2$), -2.74 (s, 2H, N**H** porphyrin ring); $^{13}$C NMR (DMSO-d6); δ ppm: 144.89, 134.64, 132.88, 131.45, 129.86, 127.78, 119.08, 112.41; CHNS analysis (%): theoretical data for $C_{44}H_{34}N_8$; C, 78.32; H, 5.08; N, 16.61; found: C, 78.30; H, 5.07; N, 16.64; UV-Vis. $\lambda_{max}$ (in acetone, nm): (Soret) 427, (Q bands) 521, 565, 592, 660 (Table 1).

**TAPFA, 2:** FTIR: (KBr) $\gamma cm^{-1}$: 3515 (NH amide str.), 3315 ($NH_2$ str.), 1705 (C=O carboxylic acid), 1643 (C=O, amide), 1595 (N-H deformation), 1476 (C=C aromatic); $^1$H NMR (DMSO-d6); δ ppm: 10.65 (s,1H,N**H**$_2$ sec-amide folic acid petridinone, Ha"), 9.97 (s,1H, N**H** sec-amide newly formed with porphyrin ring), 8.86-8.92 (m,8H, β pyrrole), 8.67 (s, 1H, H petridinone, folic acid), 8.10 (d, 7.20 Hz, 1H, N**H** aliphatic sec-amide folic acid), 7.97 (d, 5.60 Hz, 2H, ortho –phenyl to newly formed amide ), 7.81 (d, 6.40 Hz, 6H, protons on the amino phenyl rings, ortho to the porphyrin ring), 7.63 (d, 8.40 Hz, 2H, para-substuted phenyl of folic acid next to the carbonyl), 7.30 (d, 5.60 Hz, 2H, meta – phenyl to newly formed amide), 7.11 (d, 6.40 Hz, 6H, protons on the amino phenyl rings, meta to the porphyrin ring), 6.96 (t, 1H,-CH2-N**H**- folic acid), 6.58 (d, 8.40 Hz, 2H, para-substuted phenyl of folic acid next to the amine),5.78 (m, 2H, N**H**$_2$ amine folic acid), 5.58 (bs, 6H, N**H**$_2$ porphyrin ring), 4.54 (d, 4.00Hz,2H, C**H**$_2$NH folic acid), 4.36(m, 1H, C**H** folic acid next to the carboxylic acid), 2.29 (t, 2H, C**H**$_2$COOH folic acid), 1.78-2.05 (m, 2H,-COOH-$CH_2$-C**H**$_2$- folic acid), -2.79 (s, 2H, N**H**, porphyrin ring); $^{13}$C NMR (DMSO-d6); δ ppm: 173.52, 167.10, 165.36, 161.13, 156.00, 153.58, 150.11, 148.45, 145.65, 134.40, 132.67, 131.31, 129.72, 128.66, 127.68, 127.23, 121.19, 112.43, 111.07, 51.19, 45.68, 31.34, 26.69; CHNS analysis (%): theoretical

data for $C_{63}H_{51}N_{15}O_5$; C, 68.90; H, 4.68; N, 19.13; found: C, 68.93; H, 4.69; N, 19.14; UV-Vis. $\lambda_{max}$ (in actone, nm): (Soret) 429, (Q bands) 522, 565, 593, 660 (Table 1).

**TAP-Schiff base, 3:** FTIR: (KBr) $\gamma cm^{-1}$: 3420 (NH amine, str.), 3363 (NH), 1640 (C=N, imine, str.), 1600 (NH def. porphyrin), 1433 and 1400 ($N(CH_3)_2$ def.); $^1H$ NMR (DMSO-D6): δ ppm: 8.84-8.78 (m, 8H, β pyrrole), 8.52 (s, 1H, N=C**H**), 7.75 (d, J= 7.20 Hz, 6H, protons on the amino phenyl rings, ortho to the porphyrin ring), 7.60 (d, J=6.80 Hz, 2H, meta –phenyl to newly formed amide), 7.36 (d, J=7.20 Hz, 2H, protons on 4-dimethylaminophenyl ring), 7.00-7.10 (m, 8H, porphyrin proton), 6.61 (d, J= 7.20 Hz, 2H, protons on 4-dimethylaminophenyl ring), 5.58 (s, 6H, $NH_2$), 2.99 (s, 6H, $N(CH_3)_2$), -2.77 (s, 2H, N**H** pyrrole); CHNS analysis (%): theoretical data for $C_{53}H_{43}N_9$; C, 78.98; H, 5.38; N, 15.64; found: C, 78.90; H, 5.40; N, 15.60; UV-Vis. $\lambda_{max}$ (in actone, nm): (Soret) 466, (Q bands) 525, 566, 602, 661 (Table 1).

**ZnTAP, 4**: FTIR: (KBr) $\gamma cm^{-1}$: 3364 (N-H, str.), 3032 (C-H, str. Aromatic), 1600 (N-H deformation), 1471 (C=C, aromatic), 965 (Zn-N); UV-Vis. $\lambda_{max}$ (in acetone, nm): (Soret) 430, (Q bands) 560, 604 (Table 1).

**FeTAP, 5**: FTIR: (KBr) $\gamma cm^{-1}$: 3360 (NH2, str.), 3030 (C-H, str. Aromatic), 1595 (N-H deformation), 1469 (C=C, aromatic), 995 (Fe-N); UV-Vis. $\lambda_{max}$ (in acetone, nm): (Soret) 429, (Q bands) 543, 585 (Table 1).

**ZnTAPFA, 6**: FTIR: (KBr) $\gamma cm^{-1}$: 3339 ($NH_2$ str.), 1702 (C=O carboxylic acid), 1641 (C=O, amide), 1593 (N-H deformation), 996 (Zn-N); UV-Vis. $\lambda_{max}$ (in acetone, nm): (Soret) 432, (Q bands) 550, 590 (Table 1).

**ZnTAP-Schiff base, 7**: FTIR: (KBr) $\gamma cm^{-1}$: 3363 (NH), 1640 (C=N, imine, str.), 1600 (NH def. porphyrin), 1433 and 1400 ($N(CH_3)_2$ def.), 994 (Zn-N); UV-Vis. $\lambda_{max}$ (in acetone, nm): (Soret) 475, (Q bands) 530, 580 (Table 1).

**FeTAPFA, 8**: FTIR: (KBr) $\gamma cm^{-1}$: 3319 ($NH_2$ str.), 1703 (C=O carboxylic acid), 1642 (C=O, amide), 1601 (N-H deformation), 996 (Fe-N); UV-Vis. $\lambda_{max}$ (in acetone, nm): (Soret) 431, (Q bands) 530, 580 (Table 1).

**FeTAP-Schiff base, 9**: FTIR: (KBr) $\gamma cm^{-1}$: 3363 (NH2), 1642 (C=N, imine, str.), 1600 (NH def. porphyrin), 1432 and 1402 ($N(CH_3)_2$ def.), 994 (Fe-N); UV-Vis. $\lambda_{max}$ (in acetone, nm): (Soret) 468, (Q bands) 528, 570 (Table 1).

## DISCUSSION

In the FTIR spectra, all compounds revealed an absorption band around 3300-3500 $cm^{-1}$ for stretching vibration of N-H bond and 1600 $cm^{-1}$ as typical bending vibrational band of the porphyrin group. Beside these frequencies, the absorption bands belonging to C=O, C=N, C=C, and stretching vibration bands of the desired derivatives (folate and Schiff base) appeared around 1600 – 1705 $cm^{-1}$ and 1450-1470 $cm^{-1}$ respectively. Furthermore, the presence of vibrational absorption bands for Zn-N and Fe-N around 990 $cm^{-1}$ is valuable proofs for the synthesis of metalloporphyrin (28).

In the $^1H$ NMR spectra of all final porphyrin structures except metalized porphyrins, the presence of N-H pyrrole signal in the upmost filed area of the spectra around -2.76 ppm is a good evidence for the accuracy of the structures. Furthermore, the other related signals in the aromatic region comprising couple of doublet peaks for para substituted phenyl groups of TAP, TAPFA and TAP-Schiff base and β pyrrole proton signals around 9 ppm beside the specific signals of FA in the region of 4 and 2 ppm of the spectra and the singlet signal of -CH=N- segment of TAP-Schiff base in 8.50 ppm are valuable supporting evidences to confirm the synthesis of titled compounds. The symmetrical structure of TAP makes it easy to describe the simplicity and multiplicity of the $^{13}C$ NMR spectral peaks for this compound. This special feature of the spectrum which is a reliable confirmation for this synthesis has also been reported in similar reports (18,29-31).

In the $^{13}C$ NMR spectrum of TAP, 8 spectral lines related to the eight different kinds of carbons in the structure could be observed. Attachment of FA to TAP decreases the structural symmetry resulting in 23 signals in $^{13}C$ NMR spectrum as seen for TAPFA. The $^{13}C$ NMR spectra of TAPFA with 23 distinct signals confirm the attachment of FA to TAP with its aliphatic carbon signals in up field area beside the other down field peaks

belonging to the different types of carbonyl carbons in the FA structure. In overall, all $^{1}H$ NMR, $^{13}C$ NMR spectral signals and FT-IR absorption bands were in accordance with the proposed structures. In a closer investigation, we evaluated the chemical structures through CHNS analysis and in all cases the theoretical results were in a good agreement with the experimental data which can easily confirm the chemical structures of proposed porphyrins. Additionally, all porphyrins and related metalated derivatives were studied by UV-Vis spectroscopy and the spectral data are listed in Table 1 for the sake of comparison.

By comparing the results obtained for the UV-Vis spectral analysis, it can be concluded that the particular result of highly conjugated porphyrin structure is its typical electronic absorption spectrum. A typical porphyrin contains a very strong absorption around 400 nm of light spectrum known as the Soret band represents the $S_0 \rightarrow\rightarrow S_2$ transition, and several weaker absorptions between 450 and 700 nm known as the Q band indicating the $S_0 \rightarrow\rightarrow S_1$ electronic transition. The Q band consists of multiple peaks corresponding to different vibrational modes. The second excited singlet state ($S_2$) can decay to the first excited singlet state ($S_1$) and afterwards undergo intersystem crossing to the first excited triplet state (Fig. 1) (32). Due to the relatively stable triplet state and excellent triplet quantum yield, most porphyrins have known as efficient singlet oxygen photosensitizers (33). While replacement of the exterior substituents on the porphyrin ring often cause minor changes to the intensity and wavelength of the absorption bands (entries **1,2**), protonation of two of the inner nitrogen atoms or the insertion/change of metal atoms into the core of porphyrin usually intensely change the visible absorption spectrum (entries **2 and 6**). Then the Q band underwent major changes as a result of metallation (entries **4-9**). As Table 1 indicates, the most notable difference between all derivatives is the fact that the freebase porphyrins have 4 peaks in the Q band and the metalloporphyins has only 2 peaks. By comparing the UV-Vis data in Table 1, it can be realized that there are 3 or 4 absorption bands considered as Q bands and the maximum wavelength absorption (λ max) as the Soret band for all porphyrins. When the metal ion was inserted into the porphyrin ring and then coordinated with four N atoms, the number and intensity of the Q bands decreased and a slightly red shift occurred in the Soret band (e.g. TAP to ZnTAP from 427 nm red shift to 430 nm), which is the characteristic of metalloporphyrin compounds. This effect has been observed in many similar published articles and refered to as metal effect (34). The reason can be attributed to the change in structural symmetry of the metlloporphyrins. As a result, the energy gap between molecular orbitals decreased comparing to the free base porphyrins and therefore, the electron excitation needed lower energy (longer wavelength) to occur. As we can see in Table 1, during the synthesis of porphyrin-Schiff base (TAP-Schiff base) compare to the original porphyrin, a red shift in the Soret band can be observed. The presence of $NH_2$ electron-donating groups affects the energy level of molecular orbitals and any substitution that affects these energy levels can alter the photophysical properties of the product. In this regard, any substitution such as 4-dimethylamino benzaldehyde through the reaction with the amine group and formation of imine bond can improve the electron delocalization and decrease the energy gap between the π and π* where the π-π* electron excitation of the porphyrin ring requires absorbing the light of smaller energy (longer wavelength). Accordingly, the absorption band (Soret band) occurred at redshift and located in the longer wavelength region. This is exactly what we have been looking for to increase TPA cross section which is in full agreement with other reports (34). On the other hand, TPAFA did not exhibit any further delocalization compared to the original porphyrin (TPA), therefore, the slight redshift occured can be resulted from electron withdrawing ability of FA by decreasing the electron density of the porphyrin ring. Thus, the energy levels of π molecular orbitals increased and the orbital distance between highest occupied molecular orbital (HOMO)

and lowest unoccupied molecular orbital (LUMO) of the porphyrin ring became smaller and therefore the slight redshift observed (28). Another unique feature of the prepared metalloporphyrins is their improved water solubility making them promised compounds in PDT as sensitizers.

## CONCLUSION

Here, we introduced practical and concise synthesis of some porphyrin conjugates (TAP, TAPFA, TAP-Schiff base and their metalized derivatives) via the simple and efficient routes. These porphyrin derivatives revealed the acceptable spectral details as desired and due to their unique chemical and physical properties have a good potential to serve as sensitizers in PDT of cancers. Notable features of our synthesis approaches are the use of simple precursors, the experimental simplicity, ease of product isolation and good recovery yields for the porphyrin conjugates. Furthermore, the good water solubility of prepared metalloporphyrins as a main critical property for biological applications is another notable achievement of this study.

## ACKNOWLEDGMENT

The support of the School of Pharmacy and Pharmaceutical Sciences, Isfahan University of Medical Sciences, Isfahan, Iran is greatly appreciated.

## REFERENCES

1. Drain CM, Russell KC, Lehn JM. Self-assembly of a multi-porphyrin supramolecular macrocycle by hydrogen bond molecular recognition. Chem. Commun. 1996;3:337-338.
2. Haber J, Matachowski L, Pamin K, Poltowicz J. The effect of peripheral substituents in metalloporphyrins on their catalytic activity in Lyons system. J Mol Catal A Chem. 2003;198:215-221.
3. Zakharieva O, Trautwein AX, Veeger C. Porphyrin-Fe(III)-hydroperoxide and porphyrin Fe(III)-peroxide anion as catalytic intermediates in cytochrome P450-catalyzed hydroxylation reactions: a molecular orbital study. Biophys Chem. 2000;88:11-34.
4. Kessel D. Relocalization of cationic porphyrins during photodynamic therapy. Photochem Photobiol Sci. 2002;1:837-840.
5. Henderson BW, Dougherty TJ. How does photodynamic therapy work? Photochem Photobiol. 1992;55:145-157.
6. Kudinova NV, Berezov TT. Photodynamic therapy of cancer: search for ideal photosensitizer. Biomed. Khim. 2010; 55: 558-569.
7. Dewaele M, Maes H, Agostinis P. ROS mediated mechanisms of autophagy stimulation and their relevance in cancer therapy. Autophagy. 2010;6:838-854.
8. James NS, Ohulchanskyy TY, Chen Y, Joshi P, Zheng X, Goswami LN, *et al*. Comparative tumor imaging and PDT efficacy of HPPH conjugated in the mono- and di-forms to various polymethine cyanine dyes: part – 2. Theranostics. 2013;3:703-718.
9. Vicente MG. Porphyrin-based sensitizers in the detection and treatment of cancer: recent progress. Curr Med Chem. Anticancer Agents. 2001;1:175–194.
10. Karotki A, Kruk M, Drobizhev M, Rebane A, Nickel E, Spangler C W. Efficient singlet oxygen generation upon two-photon excitation of new porphyrin with enhanced nonlinear absorption. IEEE J Sel Top Quantum Electron. 2001;7:971-975.
11. Low PS, Henne WA, Doorneweerd DD. Discovery and development of folic-acid-based receptor targeting for imaging and therapy of cancer and inflammatory diseases. Acc Chem Res. 2008;41:120-129.
12. Wang S, Low PS. J. Folate mediated targeting of anti-neoplastic drugs, imaging agents and nucleic acid to cancer cells. J Control Release. 1998;53:39-48.
13. Lu Y, Low PS. Folate-mediated delivery of macromolecular anticancer therapeutic agents. Adv Drug Delivery Rev. 2002;54:675-693.
14. Pinhassi RI, Assaraf YG, Farber S, Stark M, Ickowicz D, Drori S, *et al.* Arabinogalactan−folic acid−drug conjugate for targeted delivery and target-activated release of anticancer drugs to folate receptor-overexpressing cells. Biomacromolecules. 2010;11:294-303.
15. Leamon CP, Reddy JA. Folate-targeted chemotherapy. Adv Drug Del Rev. 2004;56: 1127-1241.
16. Allen TM. Ligand-targeted therapeutics in anticancer therapy. Nat Rev Cancer. 2002;2: 750-763.
17. Li D, Diao J, Wang D, Liu J, Zhang J. Design, synthesis and biological evaluation of folate-porphyrin: a new photosensitizer for targeted photodynamic therapy. J Porphyrins Phthalocyanines. 2010;14:547-555.
18. Schneider R, Schmitt F, Frochot C, Fort Y, Lourette N, Guiillemin F, *et al*. Design, synthesis, and biological evaluation of folic acid targeted tetraphenylporphyrin as novel photosensitizers for selective photodynamic therapy. Bioorg Med Chem. 2005;13:2799-2808.
19. Milanesio ME, Alvarez MG, Durantini EN. Methoxy phenylporphyrin derivatives as

photodynamic agents. Curr Bioact Compd. 2010;6: 97–105.
20. De Visser SP, Valentine JS, Nam W. Biomimetic ferric hydroperoxoporphyrin intermediate. Angew Chem Int Ed Engl. 2010;49;2099–2101.
21. Rocha Gonsalves AMA, Serra AC, Pineiro M. The small stones of Coimbra in the huge tetra pyrrolic chemistry building. J Porphyr Phthalocyanines. 2009;13:429–445.
22. Maeda C, Kamada T, Aratani N, Osuka A. Chiral self-discriminative self-assembling of meso-meso linked diporphyrins. Coord Chem Rev. 2007;251:2743–2752.
23. Hori T, Nakamura Y, Aratani N, Osuka A. Exploration of electronically interactive cyclic porphyrin arrays. J Organome Chem. 2007;692: 148–155.
24. Savitsky A, Möbius K. Photochemical reactions and photoinduced electron-transfer processes in liquids, frozen solutions, and proteins as studied by multifrequency time-resolved EPR spectroscopy. Helv Chim Acta. 2006;89:2544–2589.
25. Balaban TS. Tailoring porphyrins and chlorins for self-assembly in biomimetic artificial antenna systems. Acc Chem Res. 2005;38:612–623.
26. Adachi S, Nagano S, Ishimori K, Watanabe Y, Morishima I, Egawa T, *et al*. Roles of proximal ligand in heme proteins: replacement of proximal histidine of human myoglobin with cysteine and tyrosine by site-directed mutagenesis as models for P-450, chloroperoxidase, and catalase. Biochemistry. 1993;32:241-252.
27. Nebert DW, Dalton TP. The role of cytochrome P450 enzymes in endogenous signalling pathways and environmental carcinogenesis. Nat Rev Cancer. 2006;6:947-960.
28. Vhadlure AN, Rohikar RV, Kulkarni GA, Suryavanshi AW, Mathkari SS, Mathapati SR. Synthesis and spectral characterization of Substituted Tetraphenylporphyrin Iron Chloride Complexes-Greener Approach. Int J Chem Tech Res. 2013;5:522-527.
29. Lazzeri D, Durantini EN. Synthesis of meso-substituted cationic porphyrins as potential photodynamic agents. 2003;2003: 227-239.
30. Wang K, Fu ST, Zhang Z, Li ZY. Synthesis and nuclear magnetic resonance shielding effect of three triazine-linked porphyrin compounds. J Braz Chem Soc. 2007;18:911-915.
31. Schiavona MA, Iwamoto LS, Ferreira AG, Iamamoto Y, Zanoni MVB, Assis MD. Synthesis and characterization of a novel series of meso (nitrophenyl) and meso (carboxyphenyl) substituted porphyrins. J Braz Chem Soc. 2000;11:458-466.
32. Smith BM. Catalytic methods for the destruction of chemical warfare agents under ambient conditions. Chem Soc Rev. 2008,37,470–478.
33. Vanessa AO, Antonio CSA, Dalva LAF, Carla MSM. Molecular modeling and UV–Vis. spectroscopic studies on the mechanism of action of reversed chloroquine (RCQ). Bioorg Med Chem Lett. 2011;21:250–254.
34. Karl M. Kadish, Kevin M. Smith, Roger Guilard. The porphyrin handbook. Texas: Elsevier science academic press; 1999.